Study of Kinetics and Macroinitiator Efficiency in Surface-Initiated Atom-Transfer Radical Polymerization

Michael R. Tomlinson,† Kirill Efimenko, and Jan Genzer*

Department of Chemical & Biomolecular Engineering, North Carolina State University, Raleigh, North Carolina 27695-7905

Received August 15, 2006; Revised Manuscript Received October 25, 2006

ABSTRACT: Generation of surface-tethered block copolymer brushes with well-defined physicochemical characteristics requires achieving good control over the degree of polymerization of each block of the copolymer. In order to precisely form these block copolymer layers, one must (1) utilize a polymerization scheme that is capable of generating nearly monodisperse polymers, (2) fully characterize the kinetics of surface-initiated polymerization, and (3) produce macroinitiators with living characteristics capable of reinitiating the growth of each subsequent block. In this work, we describe technological steps leading to the controlled growth of surface-tethered homopolymers and multiblock copolymers via surface-initiated atom transfer radical polymerization (ATRP) from flat substrates. We first report on investigating the ability of a macroinitiator to reinitiate a homopolymer brush. We use computer simulations to illustrate the advantages of an "added deactivator" type ATRP over the traditional "sacrificial initiator" ATRP. In the section describing the formation of multiblock copolymer brushes we show that the growth of individual blocks in a multiblock copolymer brush depends on the type of macroinitiator and the type of monomer used to produce the subsequent block. We demonstrate that while poly(methyl methacrylate) and poly(2-hydroxyethyl methacrylate) form multiblock copolymer brushes readily (up to a hexablock reported herein), achieving good control over growth of surface-tethered multiblock copolymers comprising poly(methyl methacrylate) and poly(dimethylaminoethyl methacrylate) blocks with equal lengths of both blocks is challenging.

Introduction

The development of new materials and devices utilizing complex polymer architectures depends greatly on the ability to accurately predict and precisely tune the properties of copolymer films. Some applications are based on di-, tri-, and multiblock copolymers in order to take advantage of the diversity of complex morphologies not encountered in classical homopolymers or polymer blends. For instance, new copolymer-based solar cells have been conceptualized, in which the interconnected and highly tunable morphologies of block copolymers are used to tune the surface area to volume ratio of the heterojunction.[1] Ongoing research in this field aims at determining the exact effect of morphology of the heterojunction on the electrical properties of these types of films.[2,3]

For most applications, polymer films are typically spin-coated onto substrates. Controlled growth of copolymer brushes from surfaces (so-called, "grafting from" methodology) offers new avenues of forming polymeric films, permanently anchored to the substrate, whose compositions and thicknesses are fully tunable. Additionally, past studies have shown that, through annealing or selective solvent exposure, the morphologies of these tethered brush films may be specifically tuned to adopt different structures.[4−6] Growing multiblock layers directly from a surface as opposed to the classical bulk synthesis offers many advantages. These include (1) highly predictable controlled linear chain growth, (2) reduction of handling in between multiblocks (lengthy steps of precipitation and catalyst separation can easily lead to loss of living chains and lowered efficiency), and (3) the formation of permanent chemical bonds to the surface, thus facilitating postpolymerization solvent washing or annealing.

In order to generate surface-anchored copolymer films with well-defined physicochemical characteristics and highly tunable morphologies, one must achieve good control over the thickness of each block, determined by the degree of polymerization, within the copolymer layer. A quest after such control involves (1) utilization of a polymerization scheme that is capable of generating polymers that are nearly monodisperse, (2) full characterization of the surface-initiated growth kinetics, and (3) formation of macroinitiators with living characteristic for each subsequent block.

In this work, we describe technological steps leading to the controlled growth of tethered multiblock copolymers via surface-initiated atom transfer radical polymerization (ATRP).[7−9] While many groups have synthesized and studied block copolymer brushes via ATRP,[5,10−12] to the best of our knowledge, there has only been one systematic study of brush macroinitiator reinitiation efficiency.[13] We commence by studying the macroinitiator capability of reinitiating the growth of a homopolymer brush. We also illustrate through experiment, supported by computer simulation, and previous research,[14,15] the advantages of an "added deactivator" type of ATRP over the traditional "sacrificial initiator" ATRP. Finally, we describe experiments designed to prepare multiblock copolymers tethered to solid surfaces. We show that control over the structure of a multiblock copolymer brush depends on the types of monomers used. Specifically, while poly(methyl methacrylate) and poly(2-hydroxyethyl methacrylate) form multiblock copolymer brushes (up to a hexablock reported herein), formation of surface-tethered copolymers comprising poly(methyl methacrylate) and poly(dimethylaminoethyl methacrylate) blocks with equal lengths of both blocks is challenging.

† Present address: Department of Physics, University of Sheffield, Sheffield, United Kingdom.

* Corresponding author. E-mail: Jan_Genzer@ncsu.edu.

10.1021/ma061885n CCC: $33.50
Published on Web 12/19/2006

Experimental Details

Deposition of the Polymerization Initiator. After chilling 20 mL of anhydrous toluene (dried over $MgSO_4$) to approximately −10 °C, 2.5 μL of (11-(2-bromo-2-methyl)propionyloxy)undecyltrichlorosilane (BMPUS) was added, which was synthesized by following previous reports.[16] A silicon wafer, cut into 1 cm × 7 cm pieces, was exposed for 30 min to UV/ozone treatment in order to generate a large number of surface-bound hydroxyl groups. The wafer was then added to the toluene solution of BMPUS and allowed to sit at −10 °C for 6 h, after which time the wafer was removed, rinsed copiously with toluene, and sonicated in pure toluene for 1−30 min (depending on the strength of the sonicator). The substrates, covered with monolayers of BMPUS, were stored in a dry box for use within a 2 week period.

Surface-Initiated Polymerization. The polymerization was carried out at 25 °C for all monomer systems, including methyl methacrylate (MMA) (99%, ACROS), 2-hydroxyethyl methacrylate (HEMA) (98%, ACROS), and dimethylaminoethyl methacrylate (DMAEMA) (98%, Aldrich). Acetone (HPLC grade, Fisher Scientific), methanol (HPLC grade, Fisher Scientific), and DI water were used as cosolvents for each monomer. Solvents and monomers were sparged with nitrogen prior to polymerizations in order to remove any oxygen. Polymerizations of MMA and DMAEMA were carried out using 50 mL of monomer, 46 mL (=1.136 mol) of methanol, 10.0 mL of deionized water, 3.0 g of bipyridine (=1.9 × 10^{-2} mol), and 9.6 × 10^{-3} mol of CuCl + $CuCl_2$ (usually in the molar ratio of 20:1).[17,18] For the PMMA−PHEMA multiblocks, it was necessary to add 7.0 mL of acetone during the polymerization of HEMA in order to solubilize the PMMA-based macroinitiator. In the case of the "sacrificial initiator" polymerization, a molar amount of ethyl-2-bromoisobutyrate (EBiB) equal to the amount of CuCl was substituted for the added $CuCl_2$ deactivator.

Continuous and "Step-Height" Polymer Brush Gradients. The polymer brush gradient-based substrates were prepared in a custom-made polymerization chamber. The chamber was continuously purged with nitrogen in order to avoid oxygenation of the macroinitiator or monomer/catalyst solutions. BMPUS-treated wafers were fixed onto a "dipping" sample holder able to control the longitudinal position of the wafer in a discrete or semicontinuous manner to less than 0.1 mm. Monomer/catalyst solutions were loaded into beakers within the chamber on a moving carousel that could be positioned below the sample. In this manner, multiple monomers could be used for a single sample run without exposing the sample or solutions to external oxygen. After each polymerization step, the wafer was immersed multiple times into a methanol solution containing dissolved bipyridine/$CuCl_2$ complex. This step was necessary in order to remove any adsorbed (but unreacted) monomer and to bring any active chains into their dormant state. Both the carousel and dipping mechanism were controlled via a computer program and a stepper motor/controller (Applied Motion Products).

Analysis of Polymer Properties. Position-dependent thickness measurements were performed with a variable-angle spectroscopic ellipsometer (VASE, J.A. Woollam). The spot size was 0.5 mm, and a constant refractive index of 1.50 was used for all polymer layers, introducing an error <3% of dry layer thickness. The molecular weight of PMMA was measured on PMMA grown in solution at a concentration of in-solution initiator that was in a molar amount much less than the amount of added $CuCl_2$. In this manner the in-solution initiator should not have contributed significantly to the [CuCl]/[$CuCl_2$] ratio. PMMA was precipitated in cold methanol, redissolved in methylene chloride, passed through an alumina column in order to remove copper residue, dried, redissolved in THF, filtered with a 0.45 μm filter, and run against PMMA standards in a size exclusion chromatograph (Waters).

Results and Discussion

Initiator Efficiency for Homopolymer "Grafting From" Polymerization. The reinitiation efficiency of a PMMA macroinitiator was examined for multiple rinse + reinitiation and growth cycles over extended periods of time (cf. Figure 1). Often there is a loss in macroinitiator activity between growing additional homopolymer or copolymer layers due to washing/handling conditions or exposure of the active layer to oxygen. In order to control/predict polymer growth, it is necessary to assess the effect of washing and collapse of the macroinitiator layer in between layer growth while minimizing exposure to oxygen. Using the polymerization apparatus described above, a "step-height" gradient of PMMA brush was created (cf. Figure 2) on a single silicon wafer. On this step height sample, 10 growth/rinse/reinitiation cycles of surface polymerization are projected. Each step is 0.5 cm in length and represents different lengths of polymerization time. In Figure 3 we plot the mean dry thickness (determined via VASE) of each step vs total polymerization time. The linearity of the thickness vs polymerization time data reveals that the growth−rinse−reinitiation cycles do not change with time and do not depend on the length of the macroinitiator. Hence, the polymerization remains controlled/"living" over long periods of time with frequent interruptions.

Many surface-initiated ATRP reactions are successfully carried out using a "sacrificial initiator" (SI) polymerization setup, in which free initiator is added to the polymerization solution, usually in a ratio equal to the activating metal complex, and the natural process of initiator bitermination results in the necessary concentration of deactivator appearing in solution to induce a well-controlled polymerization process. Previous reports indicated that "added deactivator" (AD) types of ATRP, in which deactivating metal halide is added prior to the polymerization to establish the equilibrium initially, seem to be superior in many ways to the SI polymerizations, especially for surface-confined ATRP.[14,16,19] The SI method is often used to determine whether a combination of initiator/monomer/catalyst will produce a well-controlled polymerization with polymers of well-defined molecular weight. It is our hope that our experimental results as well as the results of our computer simulations will shed more light on the potential pitfalls of using this system of measure. As will be demonstrated later in the paper, our results are in agreement with the results of Zhang and co-workers, who emphasize the importance of a small amount of deactivator added at the beginning of an ATRP process to produce lower polymers with narrow molecular weight distributions.[19]

Our previous experiment (cf. Figures 1−3) established that surface-initiated AD ATRP of MMA exhibited constant growth rate with no decrease in macroinitiator efficiency between subsequent growth/washing steps. In order to establish the difference between the SI and AD methods, a second set of experiments was designed to test and compare the effectiveness of a SI surface polymerization under similar conditions. The results are shown in Figure 4. First, a continuous PMMA thickness gradient was created by slightly immersing a 7 cm long wafer into the polymerization media with no AD and no SI present; the reaction thus begins as uncontrolled, free radical polymerization. The dipping process was started, and after 24 min (wafer position at 2.1 cm along the abscissa, cf. Figure 4) SI was added to start a controlled SI ATRP. The polymerization (now SI type) was allowed to proceed for another 60 min, while a gradient in polymer brush thickness was created on the specimen. In order to terminate the polymerization, a saturated solution of $CuCl_2$ in deoxygenated methanol was added; the wafer was then removed from the polymerization solution,

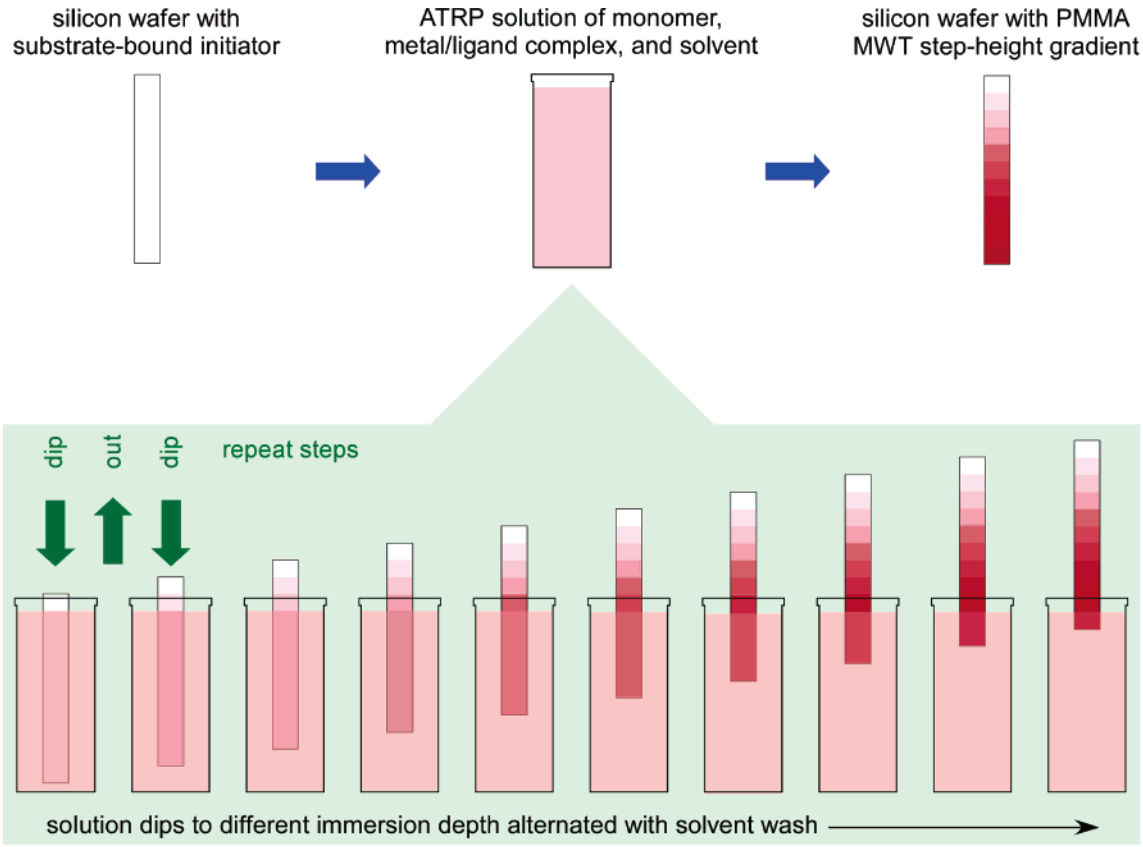

Figure 1. Technological steps leading to the formation of step-height gradients of a homopolymer brush on flat substrates. A flat silicon wafer coated with a monolayer of the polymerization initiator is vertically immersed into ATRP solution comprising monomer, metal/ligand, and solvent. After a predetermined time period, the wafer is removed from the solution and dunked onto a solvent/$CuCl_2$ mixture. After the washing step, the wafer is again immersed into the ATRP solution, such that a fraction of the originally coated substrate remains above the solution. The washing procedure as described before follows. The latter two steps (polymerization and washing) are repeated eight more times, leading to the step-height gradient comprising 10 different thicknesses of the homopolymer brush on the substrate.

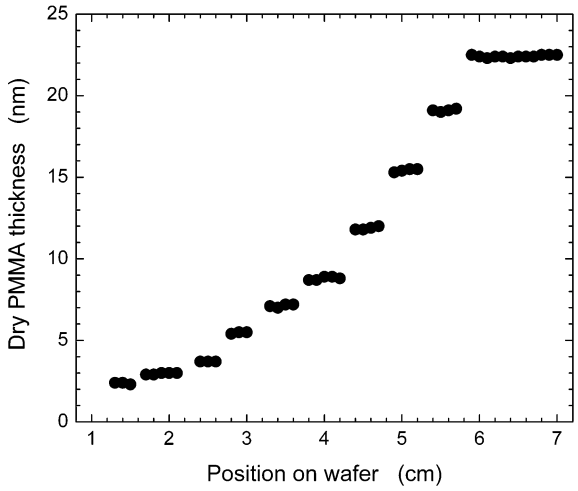

Figure 2. Dry thickness of poly(methyl methacrylate) (PMMA) as a function of the position of the substrate formed by utilizing the step-height gradient procedure outlined in Figure 1. The time steps in each dip last 45 min (dipping steps 1−3), 90 min (dipping steps 4−6), and 3 h (dipping steps 7−10). The error bars on the thickness scale are smaller than the size of the symbol.

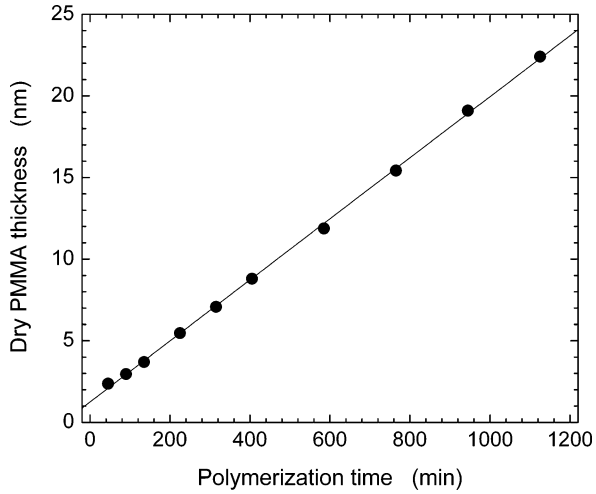

Figure 3. Dry thickness of poly(methyl methacrylate) (PMMA) as a function of the polymerization time determined from the data in Figure 2. The linear dependence of PMMA dry thickness indicates no effect of washing/collapsing brush during the multiple reinitiation steps. The error bars on the thickness scale are smaller than the size of the symbol.

rinsed with methanol and toluene, and completely dried. The resultant gradient (cf. Figure 4) was used to gather information about the surface polymerization kinetics throughout the entire growth process. During the second half of the experiment, the same gradient sample was used to initiate a second layer of PMMA in a controlled AD polymerization. The thickness change of the second layer (Δh) is governed by eq 1.

$$\Delta h = \frac{\Delta M_{\mathrm{PMMA}} \sigma}{\rho_{PMMA} N_{\mathrm{A}}} \qquad (1)$$

where ΔM_{PMMA} represents an increment in molecular weight, σ is the polymer brush grafting density on the substrate, ρ_{PMMA}

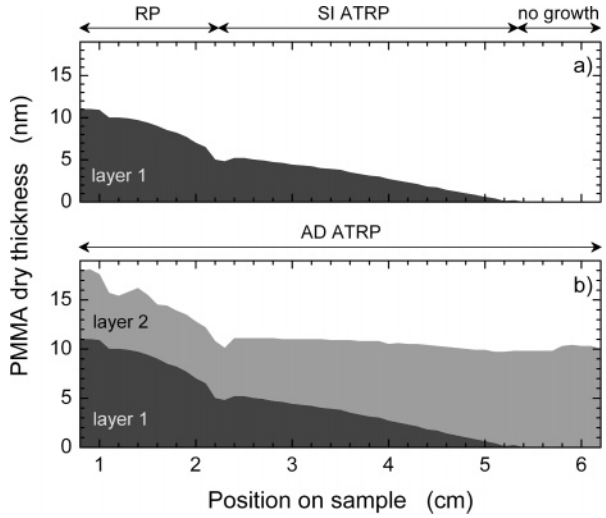

Figure 4. Dry thickness of poly(methyl methacrylate) (PMMA) as a function of the position on the substrate formed by a two-step procedure. In the first step (a), the polymerization reaction proceeds with no extra sacrificial initiator (SI) or added deactivator (AD). After 24 min into the reaction (position 2.1 cm on the wafer) a small amount of SI is added to the system (see text for details). The reaction is stopped after 60 min. (b) In the second step, a second layer of PMMA is formed by utilizing the PMMA in layer 1 formed in step 1 as a macroinitiator and immersing it into an ATRP solution containing a small amount of AD. The thickness variance in of layer 2 is assumed to be due to termination of macroinitiator.

is the density of PMMA, and N_A is Avogadro's number. Ratioing the thickness change at various positions along the sample vs the thickness change in the area of the wafer with the pure initiator layer (in Figure 4, position along wafer >5.1 cm) offers a measure of the polymer grafting density of the second block (σ_2) on the first layer relative to the grafting density of the macroinitiator layer (σ_1). This, in effect, represents the macroinitiator efficiency at any given position along the wafer. Since the change in M_{PMMA} is constant over the length of the wafer, eq 1 reduces to

$$\frac{\sigma_2}{\sigma_1} = \frac{\Delta h_2}{\Delta h_1} = \text{macroinitiator efficiency} \qquad (2)$$

A plot of this ratio over the full length of the wafer reveals that the macroinitiator efficiency, i.e., the fraction of the original growing chains that reinitiate, decreases at a fairly constant rate with increasing exposure time of the growing polymer layer to the SI polymerization media (cf. Figure 5). This decrease in efficiency is presumed to be due to chain termination arising from chain/initiator terminations. It is possible that, in this system, the radical concentration does not drop low enough to produce a well-controlled ATRP process. AD would be necessary to induce a well-controlled living process.

Computer Simulation of SI vs AD ATRP. Many research groups are studying ATRP systems both experimentally and theoretically. In the past, computer simulations have proved beneficial in providing useful insight aiming at predicting the outcomes and mechanisms of various scenarios in ATRP. Several groups have used computer simulations to predict the dependence of the number-average molecular weight (M_n) on polymerization time for various monomer/catalyst systems in ATRP.[20,21] All these models are quite similar in how they operate due to the fact that ATRP can be modeled using several fairly simple reaction equilibria. Some limitations of such approaches stem from the fact that not all input parameters, predominantly reaction rate constants, are not known a priori.

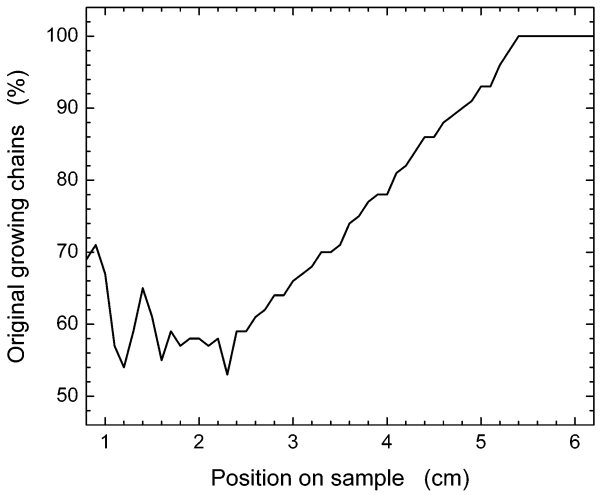

Figure 5. Percentage of growing poly(methyl methacrylate) (PMMA) chains as a function on the substrate calculated as a ratio of the position-dependent layer 2 thickness of PMMA indicated in Figure 4 and the thickness of PMMA grown via AD ATRP only.

In spite of these drawbacks, many groups are exploring computer simulation methods to obtain kinetic parameters so that more accurate models may be produced.[22−32] The relevant equations pertaining to modeling typical ATRP reaction systems are as follows:[8,33]

initiation:

$$\mathrm{I{-}X} + \mathrm{M^I X/2L} \underset{k_2}{\overset{k_1}{\rightleftharpoons}} \mathrm{I^*} + \mathrm{M^{II} X_2/2L} \qquad (3)$$

$$\mathrm{I^*} + \mathrm{M} \xrightarrow{k_i} P_1 \qquad (4)$$

propagation:

$$\mathrm{P}_n\mathrm{^*} + \mathrm{M} \xrightarrow{k_p} \mathrm{P}_{n+1}\mathrm{^*} \qquad (5)$$

$$\mathrm{P}_n\mathrm{{-}X} + \mathrm{M^I X/2L} \underset{k_d}{\overset{k_a}{\rightleftharpoons}} \mathrm{P}_n\mathrm{^*} + \mathrm{M^{II} X_2/2L} \qquad (6)$$

termination:

$$\mathrm{I^*} + \mathrm{I^*} \xrightarrow{k_{it}} \mathrm{I{-}I} \qquad (7)$$

$$\mathrm{P}_n\mathrm{^*} + \mathrm{P}_n\mathrm{^*} \xrightarrow{k_t} \mathrm{P^\circ}_{n+m} \qquad (8)$$

$$\mathrm{P}_n\mathrm{^*} + \mathrm{I^*} \xrightarrow{k_{ipt}} \mathrm{P}_n\mathrm{I} \qquad (9)$$

We used the aforementioned reactions to numerically evaluate the molecular weight and polydispersity index (PDI) of the resultant polymers by invoking a variable step-time method utilizing a second-order Runge−Kutta algorithm. Four computer simulations are discussed below; the rate constants and input values utilized in the computer simulation runs are listed in Tables 1 and 2, respectively. In Table 2 we indicate specifically which system parameters were held constant and which were being varied. The first two simulations compare end results obtained from MMA polymerizations using a CuBr/PMDETA catalyst system initiated with EBiB. The first run uses a SI system, in which no deactivator is added. In the second (the AD system), a small amount of EBiB is added along with a small amount of the deactivator. The last two runs represent systems, in which a "sluggish" initiator is used to attempt ATRP; a benzyl-type initiator would be an example for MMA polym-

Table 1. Parameters for Computer Simulation of Polymerization Kinetic

rate constant	value (L/(mol s))	action
k_1	4.3[a]	varied
k_2	4.3×10^7 [b]	varied
k_i	438[c]	constant
k_p	438[c]	constant
k_a	4.3[a]	constant
k_d	4.3×10^7 [b]	constant
k_{itt}	10^8 [d]	constant
k_t	10^8 [d]	constant
k_{ip}	10^8 [d]	constant

[a] Pintauer, T.; et al. *Macromolecules* **2004**, *37*, 2679. [b] Estimated from K_{eq}: Zhang, H.Q.; et al. *Macromolecules* **2001**, *34*, 6169−6173. [c] Matyjaszewski, K.; Davis, T. P. *Handbook of Radical Polymerization*; Wiley-Interscience: Hoboken, NJ, 2002; p 199. [d] Nikitin, A. N.; Evseev, A. V. *Macromol. Theory Simul.* **1999**, *8*, 296.

Table 2. Initial Values for Computer Simulation of Polymerization Kinetic

parameter	value (mol/L)	action
IX_0	0.047[a]	varied
M_0	9.4[a]	constant
Cu^IX	0.047[a]	constant
$Cu^{II}X_2$	0.0047[a]	varied

[a] Chatterjee, D. P.; et al. *J. Polym. Sci., Part A1* **2004**, *42*, 4132.

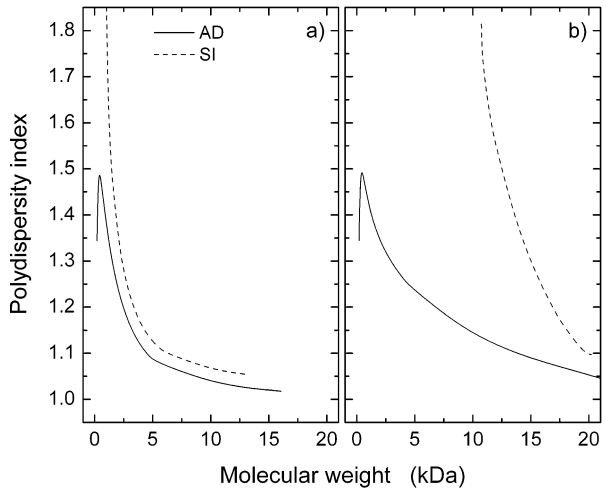

Figure 6. Polydispersity index (PDI) calculated for systems involving sacrificial initiator (SI) and added deactivator (AD) using eqs 3−9 in the text. (a) Calculation results for the PMMA CuBr/PMDETA system. PDI is noticeably higher for the SI system than for the AD system. $k_1/k_a = 1$; $k_2/k_d = 1$. (b) Calculation results for the PMMA CuCl/PMDETA system with a more sluggish initiator. As in (a), PDI is noticeably higher for the SI system than for the AD system. $k_1/k_a = 0.1$; $k_2/k_d = 4$. In all calculations we used the following molar ratios: (SI): $M_0:Cu^I_0:Cu^{II}_0:IX_0 = 200:1:0:1$, (SI + AD):$M_0:Cu^I_0:Cu^{II}_0:IX_0 = 200:1:0.002:0.1$.

erization. This computer simulation is important for mimicking the growth of block copolymers via ATRP because the first macroinitiator block can often be considered sluggish compared to the second growing block. In other words, using AD, one may be able to produce well-defined copolymers from a system that will not work well using SI ATRP.

In Figure 6a we plot the results from two computer simulations designed to model a PMMA CuBr/PMDETA system at 35 °C. The dashed lines (SI system) denote cases with added amount of in-solution initiator equal in molar amount to that of the activator (CuBr). The solid lines (AD system) denote results obtained from systems having a small amount of deactivator added at the beginning of the reaction along with only 1/10 of the molar amount of in-solution initiator. In both these simulations, initiator equilibrium (eq 3) parameters were set to be the same as the polymer equilibrium (eq 6), i.e., $k_1/k_a = k_2/k_d = 1$. The data reveal significant differences in PDIs obtained for both systems. The polymerization is more likely to run out of control during the first few minutes until enough deactivator is formed from SI termination, thereby causing an increase in PDIs early on. Because of the similar initiation and propagation terms, this effect is not significant in the first simulation. However, in the following case, the effect is made more apparent.

In Figure 6b we present the results from similar starting parameters designed to simulate a "sluggish" initiating system, i.e., phenylethyl bromide. As previously, the dashed and solid lines denote the pure SI and AD systems, respectively. In these last two simulations the initiator equilibrium (eq 3) parameters were set such that they would imitate a more sluggish phenylethyl bromide; i.e., $k_1/k_a = 0.1$, $k_2/k_d = 4$. The sluggishness of the initiator causes the system to remain uncontrolled for much longer periods of time, thereby causing much larger differenced in PDIs. Whereas the AD system could be considered to be fairly well-controlled (PDI < 1.2), the pure SI system exhibits very little control (PDI ≫ 1.2). These results agree well with the findings of Zhang and co-workers.[19] These predictive computational tools may thus be utilized to conveniently tailor any ATRP process, especially reactions involving comparatively sluggish initiators/macroinitiators.

Kinetics of PMMA Surface Polymerization. More insight into ATRP on solid substrates can be obtained by evaluating the polymerization rates as a function of the [CuCl]/[$CuCl_2$] ratio, where the value in the brackets indicates the molar concentration. Matyjaszewski, Patten, and Xia established that the rate of ATRP polymerization, R_p, is given by[8,33]

$$R_p = k_p \frac{k_a}{k_d}[\text{PMMA-Cl}][\text{MMA}]\frac{[\text{CuCl}]}{[\text{CuCl}_2]} \qquad (10)$$

where k_p is the rate constant for propagation, [PMMA-Cl] is the concentration of the growing ends of the grafted polymer, [MMA] is the concentration of the free monomer in the solution, and [CuCl] and [$CuCl_2$] are the concentrations of CuCl and $CuCl_2$, respectively. The dry thickness of PMMA on the substrate, h, is related to the polymer molecular weight, M_{PMMA}, through eq 11, which is an analogue of eq 1 mentioned earlier; hence

$$h = M_{PMMA}\frac{\sigma}{\rho_{PMMA}N_A} \qquad (11)$$

where σ is the polymer grafting density, ρ_{PMMA} is the PMMA density, and N_A is Avogadro's number. Recognizing that $R_p \sim dh/dt$ and lumping the terms that stay constant during the polymerization into a constant, one arrives at eq 12:[34]

$$\frac{dh}{dt} \sim \left(\frac{[\text{CuCl}]}{[\text{CuCl}_2]}\right)^1 \qquad (12)$$

Figure 7 depicts the dh/dt obtained by fitting the dry thickness vs polymerization time data as a function of the [CuCl]/[$CuCl_2$] ratio. Careful exploration of the data in Figure 7 reveals that the slope approaches the expected value of 1 (cf. eq 12, shown as a dashed line in Figure 7) only in the mid-$CuCl_2$ concentrations, corresponding to the [CuCl]/[$CuCl_2$] ratios ranging from 5 to 30. The growth rate at both higher and lower [$CuCl_2$] is smaller than that expected from the linear prediction in the midregion. There are two feasible explanations for this observed effect. First, at higher [$CuCl_2$] (lower value on the abscissa in

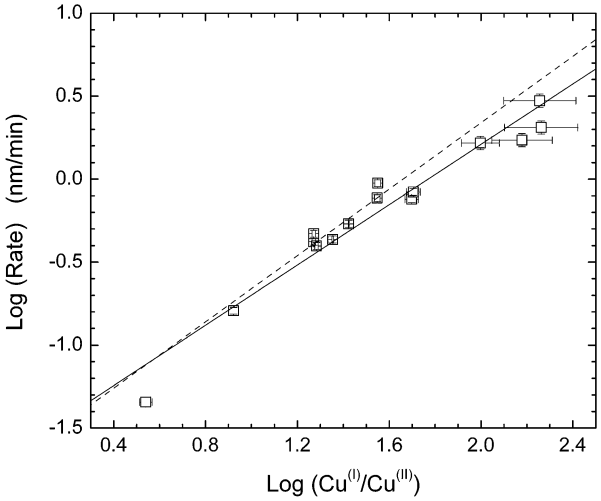

Figure 7. Surface kinetics plot for poly(methyl methacrylate) (PMMA) growth in aqueous methanol media at 25 °C. The rate is defined as the slope in the *h* vs *t* plot, where *h* is the dry thickness of the brush and *t* is the polymerization time. The dashed line represents the expected slope of 1; the solid line depicts the best fit to the data revealing a slope of 0.909. The molar ratios of MeOH:H_2O:MMA:$CuCl_2$:BiPy are 1.0:0.49:0.41:0.0085:0.0169.

Figure 7) the increased amount of $CuCl_2$, having a more positive chelating center than CuCl, can reduce the effectiveness of the in solution ligand to bind and solubilize the activating CuCl species. Second, in the regions of low [$CuCl_2$] (lower value on the abscissa in Figure 7), the reaction can become highly uncontrolled, leading to possible irreversible termination. Both these facts could cause an apparent lowering of thickness growth kinetics. While the former effect leads to a slower growth in the molecular weight vs time, the latter effect causes early irreversible termination, lowering the total "effective" grafting density of active chains. Additionally, the scaling argument shown in eq 12 is derived from the ATRP rate of polymerization that has been derived for bulk polymerization and does not take into account any constraints due to confinement effects.[35] By fitting the data (solid line in Figure 7), final estimation of the growth kinetics of PMMA in aqueous methanol media results in eq 13:

$$\log(\text{rate}) = 0.909 \log\left(\frac{[\text{CuCl}]}{[\text{CuCl}_2]}\right) - 1.607 \qquad (13)$$

where rate is the growth rate in nm/min.

In order to relate the molecular weight of grown PMMA to the surface thickness, several polymerization runs were performed at various [CuCl]/[$CuCl_2$] ratios. The in-solution initiator concentration was kept at a value that was low compared with the deactivator so as to diminish the influence on the estimated copper ratio. The results of size exclusion chromatography (SEC) analysis including the molecular weights, and PDI values are presented in Table 3.

Assuming that the molecular weight obtained from PMMA grown in solution is the same as surface-grown PMMA grown under similar conditions, we can obtain an estimation of the grafting density of the tethered PMMA.[36] Using eq 11 with known M_{PMMA}, thickness (*h*) under similar conditions, and the bulk density of PMMA (ρ_{PMMA}), we obtain an estimate of the surface grafting density of 0.25−0.35 chains/nm^2. The estimated grafting density is the highest for systems with a higher concentration of added $CuCl_2$, thus indicating more uncontrolled termination for those systems with lower amounts of added deactivator.

Table 3. Polymer Parameters from Three PMMA AD Runs[a]

[CuCl]/[$CuCl_2$]	M_n (kDa)	PDI
11	0.8	1.10
62	22	1.22
125	18	1.25

[a] The following amount of reagents were used: MMA: 50 mL (=0.467 mol), methanol: 46.0 mL (=1.136 mol), deionized water: 10 mL (=0.555 mol), bipyridine (BPY): 3.0 g (=1.92×10^{-2} mol), EBiB: 28 μL (=1.94×10^{-4} mol), [CuCl] + [$CuCl_2$] = BPY/2 = 9.6×10^{-3} mol. The molar ratio of [CuCl]/[$CuCl_2$] was varied, as indicated in the table. The reaction temperature was maintained at 25 °C.

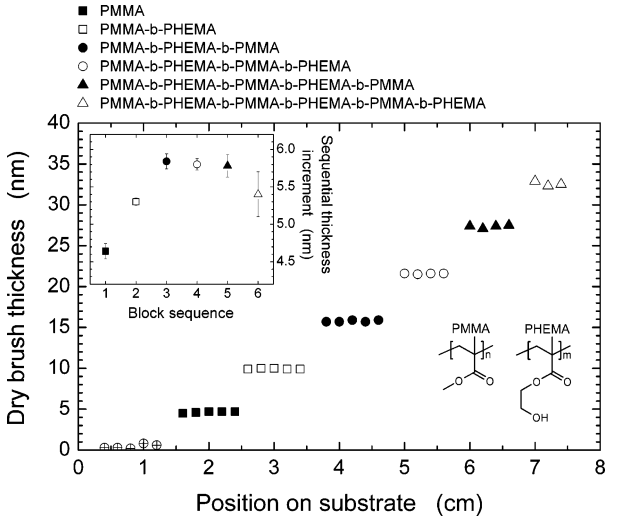

Figure 8. Dry thickness of a multiblock copolymer comprising alternating blocks of poly(methyl methacrylate) (PMMA) and poly(2-hydroxyethyl methacrylate) (PHEMA) on a solid substrate as a function of the position on the substrate. The copolymers were prepared by a variant of the method depicted in Figure 1. The growth rate of the blocks initially increases and, after reaching the second PMMA block (third block overall), approximately saturates.

Formation of Multiblock Copolymer Brushes. PMMA-*b*-PHEMA tethered multiblock copolymers were created via the "step-gradient" method described earlier. Dry thickness data from this sample are depicted in Figure 8. Because each block is grown during the same time period (45 min), we can detect the relative changes in the growth rate as the block composition changes by simply noting the growth increment. The growth increment begins at 4.6 nm long the position on the water for a pure PMMA layer and then increases to 5.3 nm as PHEMA is grown as a second block. The increment continues to increase to 5.8 nm as another PMMA block is formed and levels off at around 5.8 nm for subsequent blocks. This significant change in growth rate could be due to two effects: (1) either the PHEMA (second block) grows additional chains from the surface creating a mixed brush macroinitiator or (2) the PHEMA content increases the solubility of the macroinitiator in the aqueous methanol solution and subsequently increases the local monomer concentration at the growing polymer interface. It is highly unlikely that a mixed brush is formed. This is because the PHEMA block would have to initiate from points on the surface where PMMA chains could not grown from due to packing constraints. Not only is HEMA monomer bulkier than MMA, but the PMMA macroinitiator should be much more compact in the HEMA media since the solubility of PMMA is less in the HEMA media than the MMA media used. Therefore, another option is offered as a possible explanation of the observed effect: namely, that the increased solubility (swelling) of the macroinitiator, due to increased PHEMA content, increases the rate of growth. As multiple blocks are grown, the

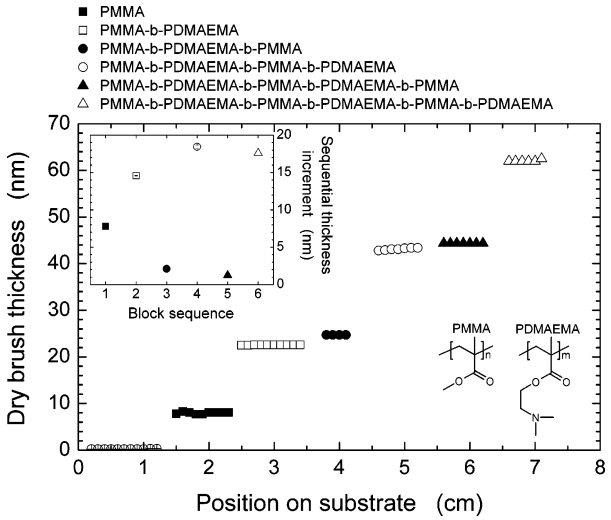

Figure 9. Dry thickness of a multiblock copolymer comprising alternating blocks of poly(methyl methacrylate) (PMMA) and poly(dimethylaminoethyl methacrylate) (PDMAEMA) on a solid substrate as a function of the position on the substrate. The copolymers were prepared by a variant of the method depicted in Figure 1. The growth rate of the PMMA block steadily decreases and saturates at small values. In contract, the growth rate of the PDAEMA increases and saturates at high values. These results indicate the low initiation efficient of PMMA from PDMAEMA and a high initiation efficiency of PDMAEMA from PMMA.

content of the macroinitiator approaches 50/50 PMMA/PHEMA, and so the growth rate levels out. If this proves to be true, this would indicate that local surface conditions can modify the kinetics at the surface relative to the bulk.

In Figure 9, the thickness of PMMA-*b*-PDMAEMA is plotted as a function of the position on the sample. It has been reported in the past that PDMAEMA could be grown from other methacrylates producing well-defined block copolymers via ATRP. However, growing other methacrylates from PDMAEMA was difficult and resulted in a significant amount of dead chains.[37] It was expected that this experiment would result in a slow decrease in growth of both blocks. However, we found out that, as the PDMAEMA thickness increased, the PMMA growth rate diminished to almost zero. The growing macroinitiator seemed to be 100% intact throughout the entire process. The chemical similarity between the two molecules suggests that they should be chemically compatible to be block copolymerized, yet the PDMAEMA macroinitiator does not transfer significantly to MMA monomer. Knowing that the PDMAEMA macroinitiators remain living throughout the entire process, we suggest a mechanism of collapse/deactivation of the PDMAEMA chain due to copper binding to the nitrogen present in DMAEMA monomer. The copper binding may not occur when sufficient amount of DMAEMA monomer is present over the growing brush, however. During the attempted growth of PMMA, the chelating monomer of DMAEMA is not present to prevent significant copper interaction with the growing chain. To this end, Guice and Loo recently reported that DMAEMA can be successfully copolymerized with HEMA, yielding a random copolymer of P(DMAEMA-*co*-HEMA) with a low PDI.[38] It thus appears that DMAEMA copolymerization with methacrylates occurs only when free DMAEMA monomer is present in the system.

Conclusions

We have described technological steps leading to the creation of step-height gradients of homopolymer and multiblock copolymer brushes on flat silicon surfaces. Using this technique, we have studied the reinitiation efficiency of PMMA homopolymer as well as multiblocks of PHEMA-*b*-PMMA. We also demonstrated that while chains terminated with PDMAEMA would not reinitiate appreciably to an MMA monomer, the activity of the growing PDMAEMA end remains intact and would continue to polymerize with a DMAEMA monomer.

We also used the technique of continuous molecular weight gradients on flat substrates to study the macroinitiator efficiency of a sacrificial initiator (SI) and added deactivator (AD) ATRP. We demonstrated that while an AD system produced linear growth with no apparent decrease in macroinitiator efficiency, an SI polymerization led to decrease in macroinitiator viability over time. This observation was partially explained by comparison with results obtained by computer modeling of an ATRP growth, which demonstrated that, in some cases, the difference in polydispersity of AD and SI polymerizations may be quite substantial. This indicates the importance of adding a small amount of deactivator to some ATRP system.[19]

Acknowledgment. We are grateful to the National Science Foundation for providing financial support for this work. We also thank the NCSU's Precision Machine Shop for their expertise in construction of the polymerization chamber.

References and Notes

(1) van Hutten, P. F.; et. al. In *Molecular Interfaces: Science and Technology for Photonic and Optoelectronic Applications*; Salaneck, W., Seki, K., Kahn, A., Pireaux, J., Eds.; Marcel Dekker: New York, 2001; pp 113−148.
(2) Moons, E. *J. Phys.: Condens. Matter* **2002**, *14*, 12235−12260.
(3) Schwartz, B. J. *Annu. Rev. Phys. Chem.* **2003**, *54*, 141−172.
(4) Zhao, B.; Brittain, W. J.; Zhao, W. S.; Cheng, S. Z. D. *J. Am. Chem. Soc.* **2000**, *122*, 2407−2408.
(5) Xu, C.; Wu, T.; Drain, C. M.; Batteas, J. D.; Fasolka, M. J.; Beers, K. L. *Macromolecules* **2006**, *39*, 3359−3364.
(6) Tomlinson, M. R.; Genzer, J. *Langmuir* **2005**, *21*, 11552−11555.
(7) Ando, T.; Kato, M.; Kamigaito, M.; Sawamoto, M. *Macromolecules* **1996**, *29*, 1070−1072.
(8) Matyjaszewski, K.; Patten, T. E.; Xia, J. H. *J. Am. Chem. Soc.* **1997**, *119*, 674−680.
(9) Matyjaszewski, K.; Xia, J. H. *Chem. Rev.* **2001**, *101*, 2921−2990.
(10) Zhao, B.; Brittain, W. *Macromolecules* **2000**, *33*, 8813−8820.
(11) Boyes, S. G.; Granville, A. M.; Baum, M.; Akgun, B.; Mirous, B. K.; Brittain, W. *Surf. Sci.* **2004**, *570*, 1−12.
(12) Börner, H. G.; Beers, K.; Matyjaszewski, K. *Macromolecules* **2001**, *34*, 4375−4383.
(13) Kim, J. B.; Huang, W.; Bruening, M. L.; Baker, G. L. *Macromolecules* **2002**, *35*, 5410−5416.
(14) Ibrahim, K.; Löfgren, B.; Seppälä, J. *Eur. Polym. J.* **2003**, *39*, 939−944.
(15) Jeyaprakash, J. D.; Samuel, S.; Dhamodharan, R.; Ruhe, J. *Macromol. Rapid Commun.* **2002**, *23*, 277−281.
(16) Matyjaszewski, K.; Miller, P. J.; Shukla, N.; Immaraporn, B.; Gelman, A.; Luokala, B. B.; Siclovan, T. M.; Kickelbick, G.; Vallant, T.; Hoffmann, H.; Pakula, T. *Macromolecules* **1999**, *32*, 8716−8724.
(17) Jones, D. M.; Huck, W. T. S. *Adv. Mater.* **2001**, *13*, 1256−1259.
(18) Chatterjee, U.; Jewrajka, S. K.; Mandal, B. M. *Polymer* **2005**, *46*, 1575−1582.
(19) Zhang, H. Q.; Klumperman, B.; Ming, W. H.; Fischer, H.; van der Linde, R. *Macromolecules* **2001**, *34*, 6169−6173.
(20) Snijder, A.; Klumperman, B.; van der Linde, R. *Macromolecules* **2002**, *35*, 4785−4790.
(21) Lutz, J. F.; Matyjaszewski, K. *Macromol. Chem. Phys.* **2002**, *203*, 1385−1395.
(22) Tang, W.; Nanda, A. K.; Matyjaszewski, K. *Macromol. Chem. Phys.* **2005**, *206*, 1171−1177.
(23) Kwark, Y. J.; Novak, B. M. *Macromolecules* **2004**, *37*, 9395−9401.
(24) Shipp, D. A.; Yu, X. *J. Polym. Sci., Part A1* **2004**, *42*, 5548−5558.
(25) Jiang, C. F.; Zhang, Y. X. *Chin. J. Chem. Eng.* **2004**, *12*, 208−213.
(26) Pintauer, T.; Braunecker, W.; Collange, E.; Poli, R.; Matyjaszewski, K. *Macromolecules* **2004**, *37*, 2679−2682.
(27) Nanda, A. K.; Matyjaszewski, K. *Macromolecules* **2003**, *36*, 599−604.

(28) Chambard, G.; Klumperman, B.; German, A. L. *Macromolecules* **2002**, *35*, 3420−3425.
(29) Matyjaszewski, K.; Paik, H. J.; Zhou, P.; Diamanti, S. J. *Macromolecules* **2001**, *34*, 5125−5131.
(30) Zhang, H. Q.; Klumperman, B.; Ming, W. H.; Fischer, H.; van der Linde, R. *Macromolecules* **2001**, *34*, 6169−6173.
(31) Matyjaszewski, K. *Macromol. Symp.* **2000**, *161*, 1−9.
(32) Coullerez, G.; Carlmark, A.; Malmstrom, E.; Jonsson, M. *J. Phys. Chem. A* **2004**, *108*, 7129−7131.
(33) Patten, T. E.; Matyjaszewski, K. *Adv. Mater.* **1998**, *10*, 901−910.
(34) Tomlinson, M. R.; Genzer, J. *Macromolecules* **2003**, *36*, 3449−3451.
(35) Genzer, J. *Macromolecules* **2006**, *39*, 7157−7169.
(36) We do not claim that this assumption is completely accurate. However, this has become a standard way to estimate the molecular weight of grafted polymer since the amount of polymer obtained from degrafting is very small, and therefore it is difficult to obtain enough material for analysis.
(37) Jin, X.; Shen, Y.; Zhu, S. *Macromol. Mater. Eng.* **2003**, *288*, 925−935.
(38) Guice, K. B.; Loo, Y. L. *Macromolecules* **2006**, *39*, 2474−2480.

MA061885N